JB Journals.ASM.org

Bacillus anthracis Acetyltransferases PatA1 and PatA2 Modify the Secondary Cell Wall Polysaccharide and Affect the Assembly of S-Layer Proteins

J. Mark Lunderberg,[a,b] Sao-Mai Nguyen-Mau,[a,b] G. Stefan Richter,[a,b] Ya-Ting Wang,[a,b] Jonathan Dworkin,[c] Dominique M. Missiakas,[a,b] Olaf Schneewind[a,b]

Howard Taylor Ricketts Laboratory, Argonne National Laboratory, Argonne, Illinois, USA[a]; Department of Microbiology, University of Chicago, Chicago, Illinois, USA[b]; Department of Microbiology and Immunology, Columbia University, New York, New York, USA[c]

The envelope of *Bacillus anthracis* encompasses a proteinaceous S-layer with two S-layer proteins (Sap and EA1). Protein assembly in the envelope of *B. anthracis* requires S-layer homology domains (SLH) within S-layer proteins and S-layer-associated proteins (BSLs), which associate with the secondary cell wall polysaccharide (SCWP), an acetylated carbohydrate that is tethered to peptidoglycan. Here, we investigated the contributions of two putative acetyltransferases, PatA1 and PatA2, on SCWP acetylation and S-layer assembly. We show that mutations in *patA1* and *patA2* affect the chain lengths of *B. anthracis* vegetative forms and perturb the deposition of the BslO murein hydrolase at cell division septa. The *patA1* and *patA2* mutants are defective for the assembly of EA1 in the envelope but retain the ability of S-layer formation with Sap. SCWP isolated from the *patA1 patA2* mutant lacked acetyl moieties identified in wild-type polysaccharide and failed to associate with the SLH domains of EA1. A model is discussed whereby *patA1*- and *patA2*-mediated acetylation of SCWP enables the deposition of EA1 as well as BslO near the septal region of the *B. anthracis* envelope.

Bacillus anthracis is a Gram-positive, spore-forming bacterium and the causative agent of anthrax (1). Following infection, spores germinate, and the resulting vegetative forms replicate in all tissues, eventually triggering the death of infected hosts (2). Spore formation in carcass tissue and contamination of the environment provide for the dissemination of the pathogen (2). To escape phagocytic clearance in host tissues, *B. anthracis* elaborates a poly-D-γ-glutamic acid (PDGA) capsule, which is tethered to cell wall peptidoglycan (3, 4). Further, bacilli form elongated chains from four or more incompletely separated cells (5). The size of *B. anthracis* vegetative chains precludes their engulfment by phagocytes (6).

The chain length of *B. anthracis* vegetative forms is controlled by proteins that are associated with the microbe's surface (S)-layer (5, 7). Two secreted proteins, surface array protein (Sap) and extractable antigen 1 (EA1), assemble into paracrystalline S-layer sheets (8, 9). Twenty-two *B. anthracis* S-layer-associated proteins (BSLs) are incorporated as minor constituents into the S-layer, where they fulfill specific functions during the pathogenesis of anthrax infections (10). For example, BslK promotes *B. anthracis* heme iron uptake (11), BslA mediates adherence of vegetative forms to host cells (12), and BslO enables separation of bacilli from elongating chains (5). Both S-layer proteins and S-layer-associated proteins are tethered to the bacterial envelope via three S-layer homology (SLH) domains, which bind to the secondary cell wall polysaccharide (SCWP) (13, 14). SLH domains fold into a three-pronged spindle structure that has been proposed to bind SCWP at the interprong grooves (15). Previous work described the SCWP of *B. anthracis* as a polysaccharide with the repeating structure [→4)-β-ManNAc-(1→4)-β-GlcNAc-(1→6)-α-GlcNAc-(1→]$_n$, where α-GlcNAc is replaced with α-Gal and β-Gal at O-3 and O-4, respectively, and the β-GlcNAc is replaced with α-Gal at O-3 (16). An SCWP strand is tethered via a murein linkage unit (GlcNAc-ManNAc, where ManNAc is *N*-acetylmannosamine) and a phosphodiester bond to the C-6 hydroxyl of *N*-acetylmuramic acid (MurNAc) within the peptidoglycan (14, 17).

The SCWP of *B. anthracis* is modified with ketal pyruvate and acetyl groups (14, 18). Pyruvylation of the SCWP requires the *csaB* gene product, which is absolutely essential for *B. anthracis* S-layer assembly (13, 14). The ketal-pyruvyl moiety is attached to the C-4 and C-6 hydroxyls of the terminal ManNAc residue in the SCWP of *B. anthracis* strain CDC 684 (18). Of note, *B. anthracis* CDC 684 is severely attenuated in the guinea pig model for anthrax disease; however, its genome sequence is closely related to that of the virulent strain *B. anthracis* Vollum (19, 20). Further, the SCWP of *B. anthracis* CDC 684 lacks the galactosyl decorations of the SCWP found in other *B. anthracis* isolates (16, 18, 21).

The SCWP of *B. anthracis* CDC 684 is acetylated at the C-3 hydroxyl of GlcNAc, the penultimate N-acetylated sugar (18). Acetylation of SCWP appears to be a universal feature of *B. anthracis* and *Bacillus cereus*, and the sites of acetylation and pyruvylation on the polysaccharide appear similar between *B. anthracis* CDC 684 and *B. anthracis* Sterne (18, 22, 23). Nevertheless, the genetic basis for such modification is not yet known. Recently, two putative acyltransferase systems, designated PatA1/PatB1 and PatA2/PatB2, were identified in *B. anthracis* and proposed to function as peptidoglycan acetyltransferases (24). PatA1 and PatA2 belong to the family of membrane-bound *O*-acyltransferases

Received 16 July 2012 Accepted 9 December 2012
Published ahead of print 14 December 2012
Address correspondence to Olaf Schneewind, oschnee@bsd.uchicago.edu.
Supplemental material for this article may be found at http://dx.doi.org/10.1128/JB.01274-12.
Copyright © 2013, American Society for Microbiology. All Rights Reserved.
doi:10.1128/JB.01274-12

TABLE 1 Bacterial strains and plasmids used in this study

Strain or plasmid	Description[a]	Reference or source
Strains		
B. anthracis		
Sterne 34F2	(pXO1$^+$ pXO2$^-$) wild type	Laboratory collection
JDB2519	*patA1*::*tetL* (Tet^r)	24
JDB2578	*patA2*::*aad9* (Spec^r)	24
JDB1972	*patA1*::*aphA3*::*patA2* (Kan^r)	24
JDB2573	*patA1*::*aphA3*::*patA2* pML360	24
JDB2609	*patA1*::*aphA3*::*patA2* pML301	24
JML145	*patA1*::*aphA3*::*patA2* pAD123	This work
B. subtilis		
PY79	Wild type	Laboratory collection
E. coli		
JWK440	BL21(DE3), pJK88	This work
Plasmids		
pML301	pAD123 derivative containing *patA2-bas0846* on a BamHI/KpnI fragment; Cm^r Amp^r	24
pML360	pAD123 derivative containing *patA1-bas0843* on a BamHI/KpnI fragment; Cm^r Amp^r	24
pAD123	pTA1060 ori, *cat* Cm^r *bla* Amp^r	35
pJK88	pET16b plasmid with the first 180 amino acids of *eag* as a translational fusion with mCherry	This work

[a] Tet^r, tetracycline resistance, Spec^r, spectinomycin resistance; Kan^r, kanamycin resistance; Cm^r, chloramphenicol resistance; Amp^r, ampicillin resistance.

(MBOAT; pfam 03062) (25), whose founding member, AlgI, was identified as a gene product required for *Pseudomonas aeruginosa* exopolysaccharide (alginate) O acetylation (26). Together with two secreted proteins, AlgF and AlgJ, AlgI is required for the transfer of acetyl groups (acetyl-coenzyme A [CoA]) from the cytoplasm, across the membrane and to the O-2 and/or O-3 positions of mannuronate residues in alginate (27). More recently, members of the MBOAT family have been proposed to function as peptidoglycan *O*-acetyltransferases (OAP), modifying the C-6 hydroxyl of MurNAc (28). Specifically, the gene for the AlgI homolog of *Neisseria gonorrhea* (*patA*) is located in a cluster with two other genes, encoding secreted proteins with esterase motifs (Ape1a and Ape2). *patA* and the Ape1a and Ape2 genes are thought to promote *N. gonorrhea* peptidoglycan acetylation via a pathway that utilizes acetyl-CoA (28–30).

The OatA membrane protein of *Staphylococcus aureus* catalyzes the O acetylation of the C-6 hydroxyl of MurNAc in peptidoglycan via its acyltransferase 3 domain (pfam 01757) (31). Homologs of *oatA* are expressed in other Gram-positive bacteria, including *B. anthracis* (24), and their products O acetylate peptidoglycan as a means to escape innate immune responses during infection (32, 33). The OatB enzyme belongs to the same family as OatA; however, OatB is thought to catalyze the acetylation of the C-6 hydroxyl of GlcNAc in peptidoglycan (34). In agreement with the general hypothesis that PatA1/PatB1, PatA2/PatB2, OatA, and OatB modify the envelope of *B. anthracis*, earlier work reported the saponified release of *O*-acetyl groups from envelope preparations in a manner requiring all of these genes (24). Nevertheless, the experimental approach used an envelope preparation comprised of peptidoglycan with the SCWP, and the possibility that PatA1/PatB1 and PatA2/PatB2 act on the SCWP, similar to AlgIJF acting on *P. aeruginosa* exopolysaccharide, can therefore not be excluded (24).

This possibility was explored here, and we report that the *patA1* and *patA2* mutant strains cannot assemble the EA1 S-layer protein in their envelopes but retain the ability of S-layer formation from Sap. Similar amounts of SCWP were isolated from *patA1 patA2* mutants. Nevertheless, the SCWP harbored fewer *O*-acetyl modifications than wild-type (WT) *B. anthracis* and failed to associate with the SLH domains of EA1. We therefore propose that PatA1/PatB1- and PatA2/PatB2-mediated O acetylation of the SCWP provides for the deposition of proteins into unique locations within the S-layer, thereby controlling the chain length of *B. anthracis* vegetative forms.

MATERIALS AND METHODS

Bacterial strains and plasmids. *B. anthracis* and *Bacillus subtilis* strains used in this study are listed in Table 1. Bacilli were cultured in brain heart infusion (BHI) broth or agar supplemented with antibiotics when necessary. Sodium bicarbonate (0.8%, wt/vol) was added to induce protective antigen (PA) and BslA expression when appropriate. *Escherichia coli* strains were grown in Luria Bertani (LB) broth. Chloramphenicol (10 μg/ml) and ampicillin (100 μg/ml) were used to maintain plasmid selection. *B. anthracis* strains were sporulated in modified G medium (modG) as previously described (36). Spore preparations were heat treated to kill any remaining vegetative bacilli and stored at 4°C. Spores were enumerated by CFU counts. Spores were germinated by inoculation into BHI medium and grown at 37°C.

Strain JWK440 is the *E. coli* BL21(DE3) strain transformed with the pJK88 plasmid containing the first 180 amino acids of EA1 as a translational fusion with mCherry. This vector was constructed by amplifying mCherry with P287 (5′-TTTCTCGAGAGCAAGGGCGAGGAGG-3′) and P288 (5′-TTTGGATCCTTACTTGTACAGCTCGTCCATG-3′) and digested with XhoI-BamHI. Cut DNA was ligated with pET16b vector DNA, also cleaved with XhoI-BamHI, and transformed into DH5α cells. The recombinant product was then digested with NdeI-XhoI and ligated with the NdeI-XhoI-cut, PCR-amplified portion of EA1 encoding the SLH domains (amino acids 30 to 210) (P289, 5′-GGAATTCCATATGGG TAAATCATTCCCAGACGTTC-3′; P288, 5′-TTTGGATCCTTACTTGT ACAGCTCGTCCATG-3′). The ligation product was transformed into *E. coli* BL21(DE3). Strain JML145 was generated by purifying pAD123 plas-

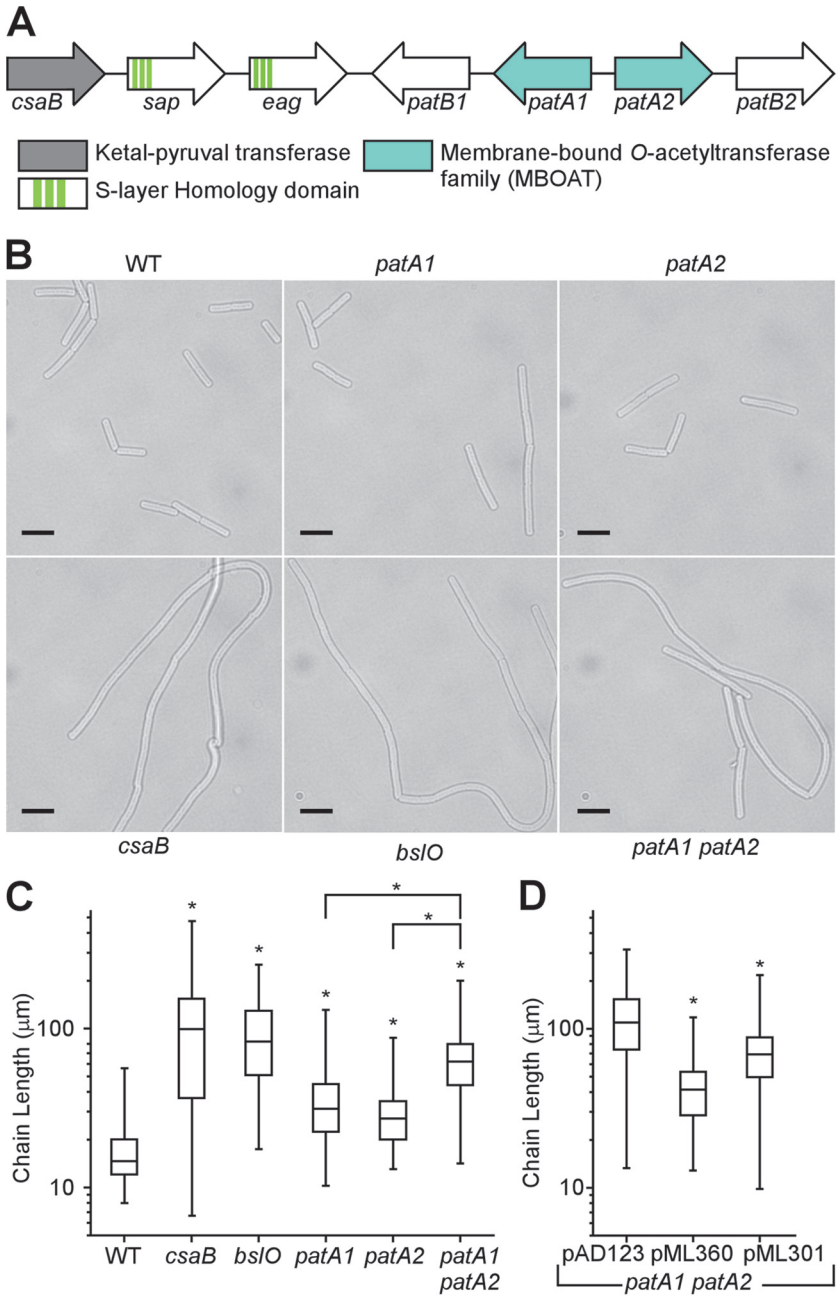

FIG 1 Mutations in the *patA1* and *patA2* genes cause chain length phenotypes in *Bacillus anthracis* vegetative forms. (A) Genes for the PatA1 and PatA2 acetyltransferases are located on the *Bacillus anthracis* chromosome immediately adjacent to genes for the major S-layer proteins (*sap* and *eag*) and to *csaB*, which encodes a ketal pyruvyl transferase essential for S-layer formation. (B) DIC microscopy images of vegetative forms germinated from *B. anthracis* wild-type and *csaB*, *bslO*, *patA1*, *patA2*, and *patA1 patA2* mutant spores. Scale bar, 10 μm. (C) The chain lengths of 100 vegetative bacilli were quantified for each strain; the data are presented as a box-and-whiskers plot, where the size of each box is defined by the boundaries of the 25th and 75th percentiles, the whiskers are the maximum and minimum measured lengths, and the center bar indicates the median length. Data were examined with an unpaired two-tailed Student's *t* test. A significant difference ($P < 0.0001$) relative to wild-type is indicated with an asterisk (*). The *patA1 patA2* mutant was also compared to mutants with singular deletions of *patA1* and *patA2* genes. (D) The *B. anthracis patA1 patA2* mutant strain was transformed with pAD123, i.e., the empty vector, pML360, a plasmid expressing *patA1-patB1*, or pML301, a plasmid expressing *patA2-patB2*. A significant difference ($P < 0.0001$) between the empty vector and the pML360 and pML301 strains was observed after data sets were compared with a Student *t* test.

mid DNA from *E. coli* K1077 (*dcm dam* mutant) and transforming JDB1972 (*patA1 patA2*) bacilli by electroporation.

Chain length of vegetative bacilli. *B. anthracis* spores were germinated by suspension in 2 ml of BHI broth at 37°C for 4 h. Cells were fixed using 4% paraformaldehyde and analyzed by microscopy. Images were obtained with a charge-coupled-device (CCD) camera on an Olympus IX81 microscope using a 100× or 40× objective. The chain lengths of bacilli were measured from acquired differential interference contrast (DIC) images using ImageJ and converted to lengths in micrometers using reference images of an objective micrometer. The statistical signifi-

cance of chain length phenotypes was analyzed using an unpaired, two-tailed Student's *t* test.

S-layer fractionation. *B. anthracis* overnight cultures, grown in BHI broth supplemented with 0.8% sodium bicarbonate (wt/vol), were diluted 1:100 into fresh medium and grown to an A_{600} of 2.5. One milliliter of culture was centrifuged at 16,000 × *g* and separated into medium (supernatant) and pellet fractions. Proteins in the medium were precipitated with 10% (vol/vol) trichloroacetic acid (TCA) for 30 min on ice and centrifuged at 16,000 × *g* for 10 min. Bacterial sediments (pellets) were washed twice with 1× phosphate-buffered saline (PBS) and boiled at 95°C for 10 min in 100 μl of PBS–3 M urea to extract S-layer and S-layer-associated proteins. Extracts were centrifuged at 16,000 × *g*, and S-layer extract was separated with the supernatant from the bacterial sediment. S-layer extract was added to an equal volume of sample buffer (4% SDS, 1% β-mercaptoethanol, 10% glycerol, 50 mM Tris-HCl [pH 7.5], bromophenol blue). The bacterial sediment was washed twice with PBS and mechanically lysed by silica bead beating for 3 min (Fastprep-24; MP Biomedical). After sedimentation of the beads, proteins in the cell lysates were precipitated with TCA and sedimented by centrifugation at 16,000 × *g* for 10 min. All TCA precipitates were washed with ice-cold acetone and dried. Samples were suspended in 100 μl of 1 M Tris-HCl (pH 8.0)–4% SDS and mixed with an equal volume of sample buffer. Aliquots (10 μl) of each sample were separated by 10% SDS-PAGE and analyzed by Coomassie staining or electro-transferred to polyvinylidene difluoride (PVDF) membranes for immunoblot analysis. Proteins were detected with rabbit antiserum raised against purified antigens. Immunoreactive products were revealed by chemiluminescent detection after incubation with horseradish peroxidase (HRP)-conjugated secondary antibody (Cell Signaling Technology). The percent amount of protein in subcellular fractions was calculated by averaging the ratio of immunoblot signals from one fraction to the sum of the signal in all fractions using three independent experimental determinations.

Purification of $EA1_{SLH}$-mCherry. One liter of LB culture of *E. coli* BL21(DE3)(pJK88) was grown at 37°C with rotation to an A_{600} of 0.6 and induced for expression of the SLH domain of EA1 fused to the fluorescent protein mCherry ($EA1_{SLH}$-mCherry) with 1 mM isopropyl-β-D-thiogalactopyranoside (IPTG) for 3 h. Cells were sedimented by centrifugation, suspended in 50 mM Tris-HCl (pH 7.5) with 150 mM NaCl and disrupted by two passages at 14,000 lb/in^2 in a French press. Lysate was cleared by centrifugation at 17,000 × *g* for 10 min to remove unbroken cells and then by ultracentrifugation at 100,000 × *g* for 30 min to sediment cell membranes. Soluble supernatant was subjected to Ni-nitrilotriacetic acid (NTA) affinity chromatography according to the manufacturer's recommendations (Qiagen). The His-tagged $EA1_{SLH}$-mCherry protein was eluted with 0.1 M imidazole, dialyzed against PBS overnight, and used for binding studies.

$EA1_{SLH}$-mCherry binding to *B. anthracis* vegetative forms. *B. anthracis* Sterne wild-type or mutant strains (*csaB*, *patA1*, *patA2*, and *patA1 patA2* strains) were grown in BHI broth to an A_{600} of 2.5, and vegetative bacilli were sedimented by centrifugation. Bacilli were suspended in PBS supplemented with 3 M urea and heated at 95°C for 10 min to solubilize the S-layer (14). Cells were again sedimented by centrifugation, washed extensively with water, and suspended in PBS. Cell density was normalized to an A_{600} of 1. These cells (100-μl samples) were then incubated with 4 μl of 15 mM $EA1_{SLH}$-mCherry for 10 min at room temperature in the dark. After incubation, cells were sedimented by centrifugation, washed extensively with PBS, and imaged by fluorescence or phase-contrast microscopy on an Olympus IX81 microscope using a 100× objective. Images were captured via a CCD camera. Alternatively, fluorescence was quantified using a Biotek Synergy HT microplate reader and 96-well format. The excitation wavelength was 590 (±20) nm, and the emission was read at 645 (±40) nm. In the SCWP inhibition assay, the $EA1_{SLH}$-mCherry protein solution was preincubated with reverse-phase high-performance liquid chromatography (rpHPLC) fractions that had been taken to dryness in a Speed-Vac and solubilized in 1 M HEPES-KOH (pH 7.5). Subsequently, 100-μl suspensions of S-layer-stripped *B. anthracis* Sterne cells (A_{600} of 1) were added. The suspension was sedimented by centrifugation, washed extensively with PBS, and quantified by fluorescence measurements as described in the $EA1_{SLH}$-mCherry binding assay. Fluorescence measurements were compared using an unpaired, two-tailed Student's *t* test.

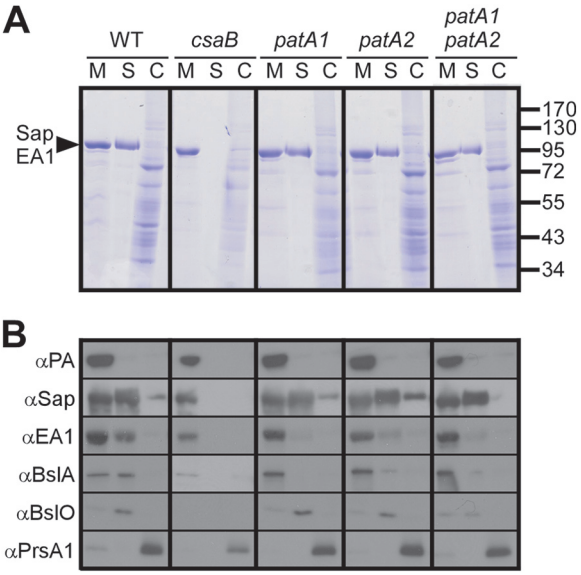

FIG 2 Impact of *patA1* and *patA2* mutations on S-layer protein and S-layer-associated protein trafficking in *B. anthracis*. (A) *B. anthracis* vegetative cultures were fractionated into medium (M), S-layer (S), and cell (C) fractions, and proteins in each sample were analyzed by Coomassie-stained SDS-PAGE gels. The arrowhead denotes the migratory position of the S-layer proteins Sap and EA1, and the numbers indicate the position of molecular mass markers (in kDa). (B) Samples generated in the experiment shown in panel A were examined by immunoblotting with antibodies raised against protective antigen (PA), a secreted protein and component of anthrax toxins (42), and PrsA1, a peptidylprolyl isomerase and membrane lipoprotein (43), as well as S-layer proteins (Sap and EA1) and S-layer-associated proteins (BslA and BslO). α, anti.

Purification of *B. anthracis* SCWP. Bacilli were grown overnight at 37°C on BHI agar, scraped off the surface, and washed in water. Bacilli were boiled for 30 min in a 4% SDS solution, washed, and suspended in water. The bacteria were mechanically lysed with 0.1-mm glass beads. The resulting murein sacculi were sedimented by centrifugation at 17,000 × *g* for 15 min, suspended in 100 mM Tris-HCl (pH 7.5), and incubated for 4 h at 37°C with 10 μg/ml DNase and 10 μg/ml RNase supplemented with 20 mM $MgSO_4$. Samples were then incubated for 16 h at 37°C with 10 μM trypsin supplemented with 10 mM $CaCl_2$. Enzymes were inactivated by boiling for 30 min in a water bath in 1% SDS. The SDS was removed by repeated cycles of centrifugation and washing in water. The murein sacculi were then washed with water, 100 mM Tris-HCl (pH 8.0), water, 0.1 M EDTA (pH 8.0), water, acetone, and finally twice with water. Murein sacculi were suspended in 5 to 7 ml of water, and 25 ml of 48% hydrofluoric acid (HF) was added. Samples were incubated overnight on ice with shaking. The acid-extracted murein sacculi were sedimented by centrifugation at 17,000 × *g* for 15 min. SCWP-containing supernatant was mixed with ice-cold ethanol in a 1:5 ratio, causing SCWP precipitation. The polysaccharide was sedimented by centrifugation at 17,000 × *g* and 4°C for 15 min, and the sediment was washed extensively with ice-cold ethanol. The SCWP was suspended in water at a concentration of 100 mg/ml, and 100 μl of this solution was subjected to rpHPLC analysis.

rpHPLC analysis was performed over a 250-mm by 4.6-mm C_{18}-ODS Hypersile column with a 3-μm-particle-size guard column (Thermos) using a water-acetonitrile gradient where the mobile phase was supple-

TABLE 2 S-layer and S-layer-associated protein distribution in *B. anthracis* wild-type and mutant strains

Protein and fraction	Amt of protein in the indicated strain (%)[a]				
	Wild type	*csaB* mutant	*patA1* mutant	*patA2* mutant	*patA1 patA2* mutant
Sap					
Medium	45 (±5)	99 (±1)	38 (±9)	37 (±4)	47 (±2)
S-layer	41 (±4)	0 (±0)	44 (±3)	41 (±5)	44 (±8)
Cell	13 (±7)	1 (±1)	17 (±9)	22 (±3)	9 (±10)
EA1					
Medium	55 (±12)	100 (±0)	85 (±5)	71 (±7)	88 (±9)
S-layer	43 (±12)	0 (±0)	12 (±4)	24 (±7)	7 (±4)
Cell	2 (±1)	0 (±0)	3 (±0)	5 (±2)	5 (±7)
BslA					
Medium	55 (±1)	100 (±0)	95 (±6)	83 (±6)	90 (±7)
S-layer	44 (±1)	0 (±0)	3 (±4)	15 (±8)	9 (±6)
Cell	1 (±1)	0 (±0)	1 (±2)	2 (±2)	1 (±1)
BslO					
Medium	19 (±6)	ND	22 (±13)	24 (±16)	55 (±10)
S-layer	77 (±9)	ND	72 (±2)	67 (±26)	45 (±9)
Cell	4 (±3)	ND	7 (±6)	10 (±10)	1 (±1)

[a] The immunoblot signals of two S-layer proteins (Sap, surface array protein, and EA1 extractable antigen 1) and two S-layer-associated proteins (BslA and BslO, S-layer-associated proteins A and O, respectively) in the medium, S-layer, and cell fraction of *B. anthracis* cultures were quantified in triplicate (Fig. 2). The mean and associated standard deviation of the percent amount in each fraction is presented here. The percentage of Sap that was retained in the S-layer did not change in strains with mutations in *patA1* or *patA2*. These strains showed defects in the S-layer retention of EA1, BslA, and BslO. ND, not detected.

mented with 0.1% trifluoroacetic acid (TFA). The gradient was derived from buffer A (water–0.1% TFA) and buffer B (acetonitrile–0.1% TFA), with a continuous flow rate of 0.5 ml per minute and the following parameters: 0 to 10 min, 0.1% buffer B; 11 to 15 min, linear gradient of 0.1 to 10% buffer B; 16 to 35 min, linear gradient of 10 to 20% buffer B; 36 to 100 min, linear gradient of 20 to 99.9% buffer B; 101 to 110 min, 99.9% buffer B. The eluate was monitored for absorbance at 206 nm, and 0.5-ml fractions were collected.

Measurement of O acetylation. Ethanol-precipitated SCWP was suspended in 25 mM sodium phosphate buffer (pH 6.5). The SCWP was treated with either 1 M or 0.01 M NaOH (final concentration) and, after 1 h at room temperature or 10 h at 4°C, samples were neutralized with the appropriate volume of 1 M HCl. For quantification of released acetate, a Megazyme Acetic Acid Kit (Megazyme International Ireland, Ltd., Wicklow, Ireland) was used according to the manufacturer's recommendations. For normalization of wild-type and *patA1 patA2* mutant SCWP concentrations, the SCWP solutions were subjected to high-performance size exclusion chromatography (HPSEC) using a 300-mm by 7.8-mm BioBasic SEC300 (Thermos) column equilibrated with 50 mM sodium phosphate buffer (pH 7.0) and a 0.1 ml/min flow rate. Chromatographs were analyzed by measuring absorbance at 206 nm. The singular peak for the SCWP was used to normalize the released acetate concentration relative to the abundance of SCWP.

MALDI-TOF mass spectrometry. rpHPLC fractions were spotted onto a Prespotted AnchorChip II, PAC II, plate (Bruker) that contained an α-cyano-4-hydroxycinnamic acid (HCCA) matrix. Calibrants were used directly from the PAC II plate. The samples were subjected to matrix-assisted laser desorption ionization–time of flight (MALDI-TOF) mass spectrometry using an Autoflex Speed Bruker MALDI instrument in positive-reflectron mode. The Bruker data analysis package was used for analysis of the spectra, and peaks were defined as having a signal-to-noise (*S*/*N*) ratio of >3.

Immunofluorescence microscopy. Spores of *B. anthracis* strains were germinated in 2 ml of BHI broth at 37°C for 3 h. Cells were sedimented by centrifugation and fixed with 4% buffered formaldehyde. Fixed samples were incubated with diluted rabbit antiserum raised against purified recombinant Sap, EA1, or BslO, and bound antibody was detected with

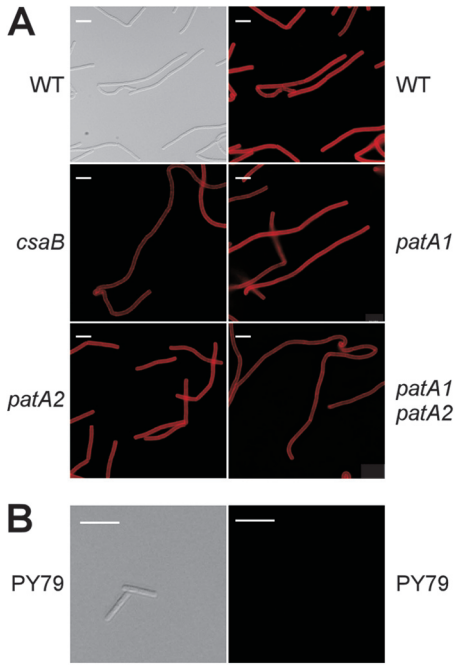

FIG 3 Mutation in *csaB*, *patA1*, or *patA2* does not alter the abundance of the SCWP in *B. anthracis*. (A) Vegetative forms derived from wild-type, *csaB*, *patA1*, *patA2*, and *patA1 patA2* mutant *B. anthracis* spores were stripped of their S-layers via treatment with 3 M urea. Bacilli were subsequently fixed with 4% paraformaldehyde and subjected either to DIC microscopy or to immunofluorescence microscopy with rabbit polyclonal antibodies raised against purified SCWP-BSA conjugate followed by secondary antibody conjugated to DyLight594. Scale bar, 10 μm. (B) *B. subtilis* strain PY79, a strain that does not elaborate an SCWP, does not show immunoreactivity toward the SCWP antibody. A refreshed overnight growth was fixed with 4% paraformaldehyde and subjected to DIC microscopy and immunofluorescence microscopy in the same manner as the *B. anthracis* strains. Scale bar, 10 μm.

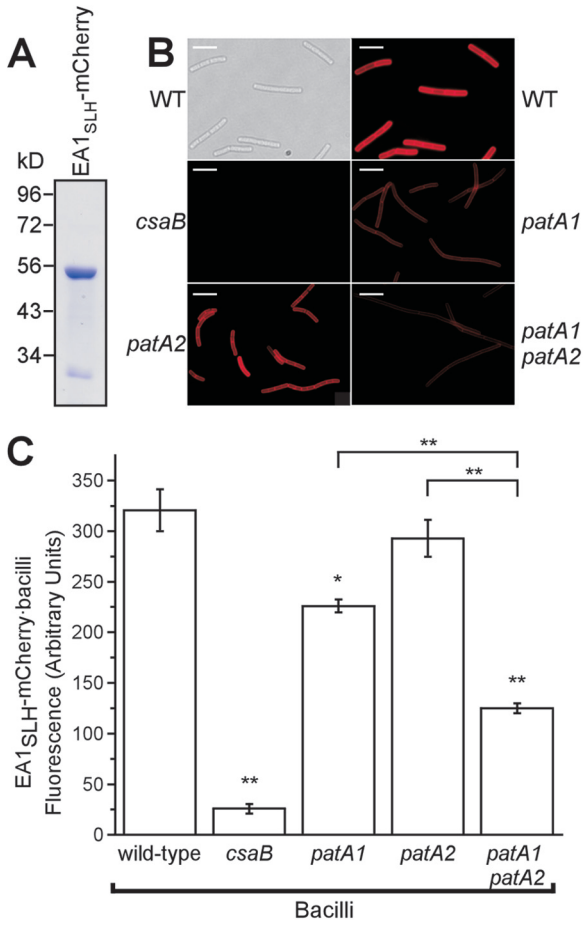

FIG 4 The SLH domain of EA1 displays reduced binding to the SCWP from *patA1 patA2* mutant *B. anthracis*. (A) Coomassie-stained SDS-PAGE gel of the purified fusion protein $EA1_{SLH}$-mCherry. Numbers indicate the positions of molecular mass markers (in kDa). (B) Vegetative forms of *B. anthracis* strains were stripped of their S-layers via treatment with 3 M urea. Differential interference contrast (DIC) and fluorescence microscopy images of the wild type and fluorescence microscopy images of *csaB*, *patA1*, *patA2*, and *patA1 patA2* mutant *B. anthracis* strains incubated with $EA1_{SLH}$-mCherry are shown. Scale bar, 15 μm. (C) The fluorescence intensity of $EA1_{SLH}$-mCherry binding to the envelope of S-layer-stripped *B. anthracis* strains was quantified in three independent experimental determinations. Data were averaged and examined with an unpaired two-tailed Student's *t* test. *, $P < 0.01$; **, $P < 0.001$.

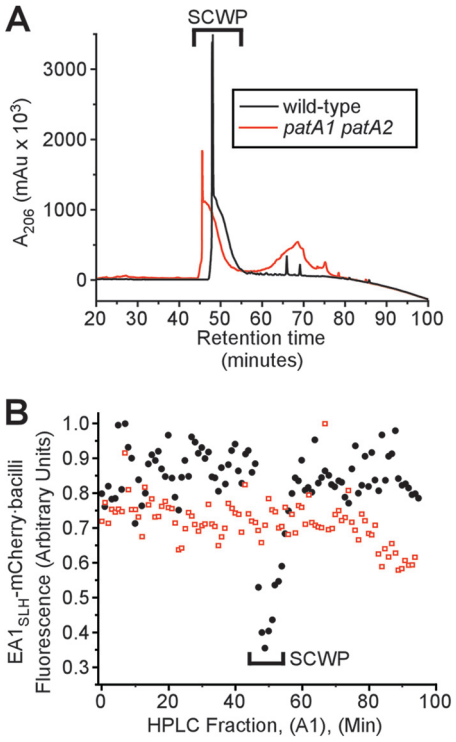

FIG 5 SCWP isolated from wild-type and *patA1 patA2* mutant *B. anthracis* strains. (A) The SCWP was released via hydrofluoric acid (HF) treatment from murein sacculi that had been isolated from either wild-type or *patA1 patA2* mutant vegetative forms. Ethanol-precipitated SCWP was subjected to rpHPLC, and the eluate's absorbance at 206 nm (A_{206}) was recorded in milli-arbitrary units (mAu). (B) Collected rpHPLC fractions from panel A (A1), were tested for competitive inhibition of $EA1_{SLH}$-mCherry binding to the SCWP of wild-type bacilli. SCWPs from wild-type but not SCWPs from *patA1 patA2* mutant bacilli displayed competitive inhibitor activities toward the binding of bacilli to $EA1_{SLH}$-mCherry.

fluorophore-conjugated secondary antibody and boron dipyrromethene (BODIPY)-vancomycin. A Leica SP5 Tandem Scanner Spectral 2-Photon confocal microscope with a 63× objective was used to observe *B. anthracis* cells.

RESULTS

Mutations in *patA1* and *patA2* cause chain length phenotypes of *B. anthracis* mutants. An important cue for the function of the *patA1* and *patB1* and the *patA2* and *patB2* genes can be derived from their location on the *B. anthracis* chromosome (Fig. 1A). The *patA1-patB1-patA2-patB2* cluster is located immediately adjacent to three genes, *csaB-sap-eag*, encoding the two S-layer proteins (Sap and EA1) and the ketal pyruvyl transferase that modifies the SCWP (CsaB). Earlier work reported that *B. anthracis patA1*, *patA2*, and *patA1 patA2* mutants, compared to wild-type bacilli, display increased chain lengths of their vegetative forms (24). Nevertheless, the chain length phenotypes have not yet been quantified. We sought to address the questions of whether the *patA1*, *patA2*, and *patA1 patA2* mutants produce variable chain lengths and how these phenotypes compare with those of *B. anthracis csaB* and *bslO* variants. Spore preparations of *B. anthracis* wild-type, *csaB*, *patA1*, *patA2*, and *patA1 patA2* strains were inoculated in BHI broth at 37°C and incubated for 4 h. The resulting vegetative forms were fixed and visualized by light microscopy, and the lengths of 100 chains were quantified (Fig. 1B and C). Wild-type bacilli displayed an average chain length of 16.9 μm. As expected, the average chain length of *csaB* and *bslO* mutant bacilli was increased to 109.0 μm and 95.2 μm, respectively (Fig. 1C) (5). The average chain lengths of strains with a deletion of the *patA1* or the *patA2* gene was moderately increased to 35.9 μm or 29.5 μm, respectively (WT versus the *patA1* strain, $P < 0.0001$; WT versus the *patA2* strain, $P < 0.0001$). The *B. anthracis patA1 patA2* mutant lacks both MBOAT acetyltransferases and displayed a further increase in average chain length (64.5 μm) (WT versus *patA1 patA2* mutant, $P < 0.0001$; *patA1* strain versus *patA1 patA2* mutant, $P < 0.0001$; *patA2* strain versus *patA1 patA2* mutant, $P < 0.0001$). Transformation of the *patA1 patA2* strain with pML360, a plasmid containing *patA1* and *patB1*, or pML301, harboring *patA2* and *patB2*, diminished the average chain length relative to transformation with the empty pAD123 vector alone (strain car-

rying pAD123 versus pML360, $P < 0.0001$; strain carrying pAD123 versus pML301, $P < 0.0001$) (Fig. 1D). These data reveal a chain length phenotype of the *patA1 patA2* mutant strain, which is, however, not as severe as the exaggerated chain length phenotypes of the *bslO* and *csaB* mutant strains (5). Further, the *patA1* and *patA2* genes fulfill complementary but not redundant roles in *B. anthracis* S-layer assembly as the mutant lacking both genes displays an additive chain length phenotype over mutants with a deletion of only one gene.

***B. anthracis patA1 patA2* mutants cannot retain EA1 in their S-layers.** Earlier work used lithium chloride extraction of *B. anthracis* S-layer proteins and analysis via Coomassie-stained SDS-PAGE gels to characterize *patA1 patA2* mutants (24). The results suggested that the *patA1 patA2* mutant, but not mutants with a deletion of only *patA1* or *patA2*, are defective in retaining S-layer proteins, presumably Sap, in the bacterial envelope (24). We used Coomassie-stained SDS-PAGE gels and immunoblotting with rabbit polyclonal antibodies, which had been raised against purified proteins, to analyze the subcellular location of S-layer proteins and BSLs in *B. anthracis* cultures fractionated into extracellular medium (M), S-layer (S), and cells (C) (Fig. 2). Unlike the *csaB* mutant, which does not assemble an S-layer, the *patA1*, *patA2*, and *patA1 patA2* mutants all assembled S-layers (Fig. 2A). Quantifying the distribution of S-layer proteins in wild-type and variant strains, we noted that the *patA1*, *patA2*, and *patA1 patA2* mutants form S-layers via Sap assembly but incorporated reduced amounts of EA1 into these structures (Table 2). As a control, wild-type and mutant bacilli secreted protective antigen (PA) into the extracellular medium and deposited PrsA1 peptidyl-prolyl-isomerase into the cytoplasmic membrane (Fig. 2B). As expected, the *csaB* mutant was unable to deposit BslA and BslO into its envelope. The *patA1* and *patA2* mutants incorporated BslO, but not BslA, into their Sap S-layers. In contrast, the *patA1 patA2* mutant was defective not only for the deposition of BslA but also for the incorporation of BslO into its S-layer. These results indicate that *patA1*, *patA2*, and *patA1 patA2* mutants form S-layers predominantly via the assembly of Sap, which suggests further that the corresponding chain length phenotypes cannot be explained as defects in the envelope assembly of Sap (37).

Mutations in *csaB*, *patA1*, and *patA2* do not affect *B. anthracis* synthesis of the SCWP. To address the question of whether there is a defect in the synthesis of the SCWP in *csaB*, *patA1*, *patA2*, and *patA1 patA2* mutant *B. anthracis* strains, we utilized a polyclonal anti-SCWP antibody to investigate the abundance and localization of SCWP in vegetative bacilli. *B. anthracis* cultures were grown in BHI broth to an A_{600} of 1, stripped of their S-layers by incubation at 95°C in phosphate-buffered 3 M urea, and fixed for immunofluorescence microscopy experiments. Rabbit polyclonal antibodies raised against SCWP-bovine serum albumin (BSA) detected the presence of SCWP in the envelope of wild-type bacilli (Fig. 3A). Neither the abundance nor the distribution of the SCWP was affected in *B. anthracis* mutants lacking the *csaB*, *patA1*, and *patA2* genes (Fig. 3A). As a control, antibodies raised against SCWP did not stain the envelope of *Bacillus subtilis*, a related spore-forming microbe that does not synthesize SCWP or S-layers (Fig. 3B).

$EA1_{SLH}$-mCherry association with the SCWP of *B. anthracis* requires *patA1* and *patA2*. To dissect the biochemical defect of *patA1 patA2* mutants, we used a previously established *in vitro* assay for S-layer assembly (14). The $EA1_{SLH}$-mCherry hybrid, which encompasses the SLH domain of EA1 fused to the fluorescent protein mCherry, was purified from the cytoplasm of *E. coli* via affinity chromatography and analyzed by SDS-PAGE (Fig. 4A). When incubated with vegetative bacilli that had been stripped of their S-layers, $EA1_{SLH}$-mCherry bound to ketal-pyruvylated SCWP in the envelope of *B. anthracis*, as visualized by fluorescence microscopy and quantified in fluorescence plate reader experiments (Fig. 4B and C). As a control, no binding of $EA1_{SLH}$-mCherry to SCWP was observed for *csaB* mutant bacilli (Fig. 4B and C). The SCWP of *patA1* but not *patA2* bacilli displayed a moderate reduction in the ability to bind $EA1_{SLH}$-mCherry (Fig. 3B and C) (WT versus the *patA1* mutant, $P < 0.001$; WT versus the *patA2* mutant, $P > 0.05$). However, the defect in $EA1_{SLH}$-mCherry binding was more pronounced in the *patA1 patA2* mutant strain than in the *patA1* mutant alone (Fig. 4B and C) (*patA1* mutant versus *patA1 patA2* mutant, $P < 0.001$).

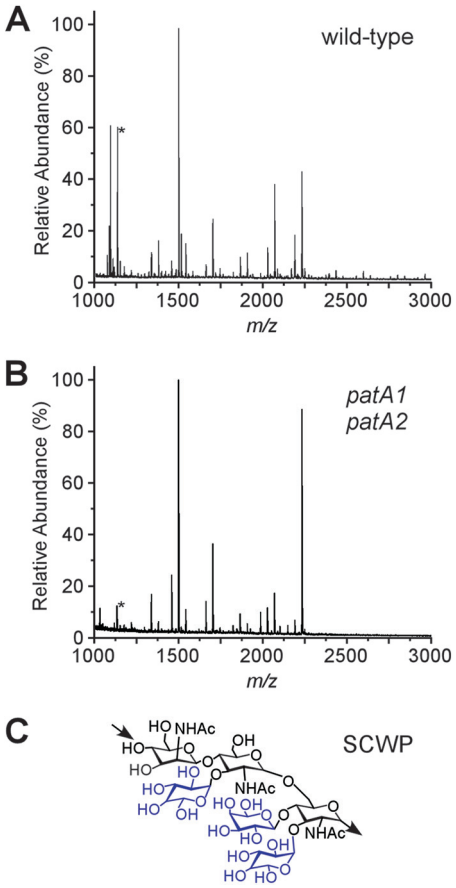

FIG 6 MALDI-TOF mass spectrometry of SCWP isolated from wild-type and *patA1 patA2* mutant *B. anthracis* strains. (A) rpHPLC-purified SCWP from wild-type *B. anthracis* was subjected to MALDI-TOF mass spectrometry, and ion spectra were recorded. *m/z*, mass-to-charge ratio. The ion signal marked with an asterisk (*) identifies the sodiated adduct of a compound with the predicted structure [β-ManNAc-(1→4)-β-GlcNAc(Gal)-(1→6)-α-GlcNAc-$(Gal)_2$]. (B) rpHPLC-purified SCWP from *patA1 patA2* mutant *B. anthracis* was analyzed by MALDI-TOF mass spectrometry, and ion spectra were recorded. (C) The SCWP is comprised of the repeating unit [→4)-β-ManNAc-(1→4)-β-GlcNAc-(1→6)-α-GlcNAc-(1→]$_n$ (printed in black), where α-GlcNAc is replaced with α-Gal and β-Gal at O-3 and O-4, respectively, and the β-GlcNAc is replaced with α-Gal at O-3 (galactosyl substitutions printed in blue) (16).

TABLE 3 Ions present in MALDI-TOF spectra of hydrofluoric acid-released SCWP from wild-type and *patA1 patA2* mutant murein sacculi of *B. anthracis* Sterne[a]

Observed *m/z* in:					
WT strain[c]	*patA1 patA2* mutant	Proposed composition[b]	Theoretical *m/z* (monoisotopic)	WT Δ*m/z*[d]	*patA1 patA2* mutant Δ*m/z*[e]
1,094.792	1,094.636	$HexNAc_2$-GlcN-Gal_3	1,094.39	−0.41	−0.25
1,136.849**	1,136.826	$HexNAc_3$-Gal_3	1,136.40	−0.45	−0.43
1,177.869	1,177.868	$HexNAc_4$-Gal_2	1,177.42	−0.45	−0.44
1,218.926	1,218.920	$HexNAc_5$-Gal	1,218.45	−0.48	−0.47
1,338.926	1,338.926	$HexNAc_4$-Gal_3	1,339.48	0.55	0.55
1,380.005	1,379.966	$HexNAc_5$-Gal_2	1,380.50	0.50	0.54
1,460.034	1,460.014	$HexNAc_3$-GlcN-Gal_4	1,459.52	−0.52	−0.50
1,500.091*	1,500.061	$HexNAc_4$-GlcN-Gal_3	1,500.55	0.45	0.48
1,542.101	1,542.114	$HexNAc_5$-Gal_3	1,542.56	0.45	0.44
1,584.103*	1,583.995	$HexNAc_6$-Gal_2	1,583.58	−0.52	−0.41
1,662.177	1,662.183	$HexNAc_4$-GlcN-Gal_4	1,662.60	0.42	0.41
1,704.213	1,704.212	$HexNAc_5$- Gal_4	1,704.61	0.40	0.40
1,746.253	1,746.257	$HexNAc_6$- Gal_3	1,745.63	−0.62	−0.62
1,824.292	1,824.292	$HexNAc_4$-GlcN-Gal_5	1,824.65	0.36	0.36
1,866.287	1,866.282	$HexNAc_5$-Gal_5	1,866.66	0.37	0.38
1,908.304*	1,908.318	$HexNAc_6$-Gal_4	1,907.69	−0.62	−0.63
1,986.422	1,986.356	$HexNAc_5$-GlcN-Gal_6	1,986.70	0.28	0.35
2,028.405	2,028.377	$HexNAc_5$-Gal_6	2,028.71	0.31	0.34
2,070.431*	2,070.403	$HexNAc_6$-Gal_5	2,069.74	−0.69	−0.66
2,232.542*	2,232.519	$HexNAc_6$-Gal_6	2,231.79	−0.75	−0.73
2,392.756	2,392.413	$HexNAc_5$-GlcN- Gal_6	2,392.86	0.11	0.45
2,434.629	2,434.629	$HexNAc_6$-Gal_6	2,434.87	0.24	0.24
2,476.694	2,476.520	$HexNAc_8$-Gal_5	2,475.90	−0.79	−0.62
2,554.825	2,554.663	$HexNAc_6$-GlcN-Gal_7	2,554.91	0.09	0.25
2,596.851	2,596.683	$HexNAc_7$-Gal_7	2,596.93	0.07	0.24
2,638.864	2,638.688	$HexNAc_8$-Gal_6	2,637.95	−0.91	−0.74
2,758.834	2,758.651	$HexNAc_7$-GlcN-Gal_7	2,757.99	−0.84	−0.83
2,800.836	2,800.651	$HexNAc_8$-Gal_7	2,800.00	−0.83	−0.65
2,920.999	2,920.999	$HexNAc_7$-GlcN-Gal_8	2,920.05	−0.95	−0.95
2,963.070	2,963.070	$HexNAc_8$-Gal_8	2,962.06	−1.01	−1.01

[a] Ion signals and proposed composition of compounds from MALDI-TOF mass spectra of rpHPLC-purified SCWPs from wild-type *B. anthracis* Sterne and the *patA1 patA2* strain.
[b] HexNAc, ManNAc (*N*-acetylmannosaminyl) and GlcNAc (*N*-acetylglucosaminyl); GlcN, glucosaminyl; Gal, galactosyl. The SCWP isolated from wild-type and the *patA1 patA2* mutant strains generated nearly identical sets of ions, similar to spectra characterizing the SCWP structure. The proposed composition was derived from sodiated, positively charged ions. Of note, additional compositional explanations for the observed masses exist; however, they are not listed here.
[c] Observed ions noted with a single asterisk (*) were accompanied by less intense ions with an additional *m/z* 15.999 and were interpreted as oxygen adducts of the parent ion. The ion noted with a double asterisk (**) was accompanied by a less intense ion with reduced *m/z* 2.011; this accompanying ion was interpreted as an oxygen adduct (+15.999) and dehydration product (−18.01) of the parent ion.
[d] Theoretical *m/z* − observed WT *m/z*.
[e] Theoretical *m/z* − observed *patA1 patA2* mutant *m/z*.

SCWP from the *B. anthracis patA1 patA2* mutant does not prevent $EA1_{SLH}$-mCherry binding to wild-type bacilli. The SCWP was released from the murein sacculi of wild-type and *patA1 patA2* mutant *B. anthracis* cells via hydrofluoric acid (HF)-mediated hydrolysis of the phosphodiester bond between the C-6 hydroxyl of MurNAc in peptidoglycan and the GlcNAc-ManNAc moiety of the murein linkage units for the SCWP. Acid-extracted polysaccharide was precipitated with ethanol and subjected to rpHPLC. Absorbance was monitored at 206 nm, and a single, large, compound peak eluted at 48 to 52 min during the chromatography of HF-extracted wild-type SCWP (Fig. 5A). Elution fractions corresponding to this absorbance peak, but not any other rpHPLC fraction, inhibited the binding of $EA1_{SLH}$-mCherry to ketal-pyruvylated SCWP in *B. anthracis* cells that were stripped of their S-layers (Fig. 5B). A similar absorbance peak at 48 to 52 min was observed during rpHPLC of HF-released SCWP from the *patA1 patA2* mutant strain (Fig. 5A). Unlike wild-type SCWP, the *patA1 patA2* mutant SCWP did not inhibit binding of $EA1_{SLH}$-mCherry to ketal-pyruvylated SCWP in vegetative bacilli (Fig. 5B).

Mass spectrometry of the SCWP from wild-type and *patA1 patA2* mutant *B. anthracis*. The SCWP of wild-type and *patA1 patA2* mutant *B. anthracis*, eluting at 48 to 52 min during rpHPLC, was subjected to MALDI-TOF mass spectrometry (Fig. 6A and B). For example, *m/z* 1,136.8 and *m/z* 2,232.5 were abundant ion signals derived from each SCWP preparation (Fig. 6). These compounds represent the sodiated adducts of one and two SCWP repeating units, respectively (Fig. 6). Table 3 summarizes ion signals from wild-type and *patA1 patA2* mutant SCWPs that were found in both samples. Sodiated ion signals conforming to variable lengths of the SCWP repeating units were abundantly present in each spectrum. Less abundant ions differed from the repeating units, in agreement with the general hypothesis of SCWP heterogeneity in galactosyl modification and acetylation. For example, *m/z* 1,500.55 conforms to a compound structure of four acetylated amino sugars and three decorating galactosyl sugars with one

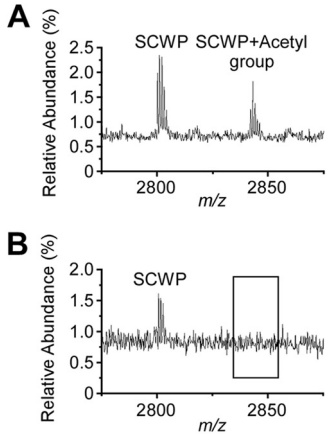

FIG 7 Ion signals for acetylated SCWP in wild-type but not in *patA1 patA2* mutant *B. anthracis* cells. (A) Ion signals from the wild-type SCWP were detected with MALDI-TOF mass spectrometry; *m/z* 2,800.7 was interpreted as the sodiated ion [ManNAc-GlcNAc$_2$(Gal$_3$)]$_2$-ManNac-GlcNAc(Gal), and *m/z* 2,842.8 was interpreted as its acetylated variant. (B) Ion signals from the *patA1 patA2* mutant SCWP were detected with MALDI-TOF mass spectrometry; *m/z* 2,800.7 was interpreted as the sodiated ion [ManNAc-GlcNAc$_2$(Gal$_3$)]$_2$-ManNac-GlcNAc(Gal). *m/z* 2,842.7 was not detected in the spectrum. Of note, although mass spectrometry data are in agreement with the proposed compound structures, they do not constitute experimental proof for the structural assignments.

deacetylated amino sugar in the repeating sequence of the SCWP (Table 3).

Both wild-type and *patA1 patA2* mutant SCWPs generated the ion signal *m/z* 2,800.7, which can be interpreted as the sodiated ion [ManNAc-GlcNAc$_2$(Gal$_3$)]$_2$-ManNac-GlcNAc(Gal) (Fig. 7A and B). Wild-type SCWP generated also *m/z* 2,842.8, which can be interpreted as the acetylated form of [ManNAc-GlcNAc$_2$(Gal$_3$)]$_2$-ManNac-GlcNAc(Gal) (Fig. 7A). On the other hand, the SCWP isolated from the *patA1 patA2* mutant did not generate *m/z* 2,842.8, suggesting that the appearance of acetylated SCWP species may require the expression of *patA1* and *patA2*. Of note, although the mass spectrometry data in Fig. 7A and B are in agreement with the proposed compound structures, they do not constitute experimental proof for the structural assignments. Similar observations were made for the ion signals *m/z* 2,680.849 and *m/z* 2,638.864 from wild-type SCWP; *m/z* 2,638.688 but not *m/z* 2,680.849 was identified in the SCWP from the *patA1 patA2* mutant strain (Table 3).

Quantification of sodium hydroxide-released acetate from wild-type and *patA1 patA2* mutant SCWP. To examine whether the SCWP of *patA1 patA2* mutant bacilli harbors fewer *O*-acetyl groups than the SCWP of wild-type *B. anthracis* cells, we extracted polysaccharides with hydrofluoric acid from the envelope of bacilli and subjected HPSEC-purified SCWP to base-catalyzed hydrolysis of *O*-acetyl groups. Released acetate was quantified via enzyme assay and normalized to the SCWP peak area during HPSEC chromatography (see Fig. S1 in the supplemental material). Compared to acetate groups released from wild-type SCWP, which were set as 100% (±3%), *patA1 patA2* mutant SCWP harbored 60% (±2%) of the 1 M sodium hydroxide-released acetate. Using a milder alkaline treatment, 0.01 M NaOH at 4°C, the *patA1 patA2* mutant SCWP harbored 45% (±0%) of the acetate released by wild-type SCWP; the wild type was again set as 100% (±1%). These data indicate that acetylation of the SCWP indeed requires the *patA1* and *patA2* genes.

Localizing S-layer proteins and BslO in the envelope of wild-type and *patA1 patA2* mutant *B. anthracis* strains. Data presented here suggest that the *patA1* and *patA2* genes promote acetylation of the SCWP, a modification that impacts the deposition of some, but not all, S-layer and S-layer-associated proteins in the envelope of *B. anthracis*. To visualize protein deposition into the S-layer, we used polyclonal rabbit antibodies raised against purified recombinant proteins for fluorescence microscopy of *B. anthracis* vegetative forms. Immunofluorescence microscopy experiments revealed incorporation of Sap into the S-layer of wild-type *B. anthracis* (see Fig. S2 in the supplemental material). Although Sap was deposited throughout the envelope of *B. anthracis*, fluorescence microscopy experiments detected areas of abundant Sap deposition near the poles but not at the cell division septa of vegetative chains (see Fig. S2). Division septa are defined as sites of intense BODIPY-vancomycin staining, a compound that binds to the precursors of peptidoglycan synthesis (see Fig S2). Deposition of Sap into the S-layer was abolished in *csaB* mutant *B. anthracis* (see Fig. S2). In contrast, deletion of *patA1* or *patA2* or of *patA1* and *patA2* did not prevent the incorporation of Sap into the S-layer. Of note, the *patA1 patA2* mutant, but not variants with a single deletion of *patA1* or *patA2*, lacked the abundant deposition of Sap near the poles of vegetative chains (see Fig. S2). This defect was rescued when plasmid pML360 (*patA2*) was transformed into the *patA1 patA2* mutant, whereas pML301 (*patA1*) had no effect.

Immunofluorescence microscopy experiments revealed the deposition of EA1 near the cell division septa of wild-type vegetative chains, similar to recently reported data (Fig. 8) (7). As expected, the *csaB* mutant did not deposit EA1 into the *B. anthracis* envelope (Fig. 8). The *patA1* and *patA2* mutant strains incorporated EA1 into the *B. anthracis* envelope; however, the fluorescent signals did not coincide with BODIPY-vancomycin staining of cell division septa (Fig. 8). In contrast, the *patA1 patA2* mutant strain failed to deposit EA1 into the S-layer of vegetative chains (Fig. 8). This defect was rescued by plasmids providing for the expression of either *patA1* or *patA2* (Fig. 8).

In agreement with earlier reports, immunofluorescence microscopy revealed the deposition of BslO near the cell division septa of wild-type *B. anthracis* vegetative chains (Fig. 9) (5). As a control, BslO deposition into the S-layer did not occur in vegetative forms of the *csaB* mutant strain (7) (Fig. 9). Both the *patA1* and the *patA2* mutant strains displayed an aberrant pattern of BslO deposition, in which the protein was detected in about half of the cell division septa of vegetative chains but was absent from the remaining septa (Fig. 9). Further, the *patA1 patA2* mutant strain deposited very little, if any, BslO near division septa (Fig. 9). This defect was rescued in part by plasmids expressing either *patA1* or *patA2* in the *patA1 patA2* mutant strain (Fig. 9).

DISCUSSION

The goal of our study was to elucidate the role of *patA1* and *patA2* in S-layer assembly and function in *B. anthracis*. Several lines of evidence suggest that *patA1* and *patA2* affect S-layer assembly. First, *patA1* and *patA2* as well as the genes for their cognate secreted acetyltransferases are located immediately adjacent to the S-layer genes (*csaB-sap-eag*) on the *B. anthracis* chromosome. Second, mutations in *patA1* and *patA2* cause a chain length phenotype, which has previously been attributed to the improper assem-

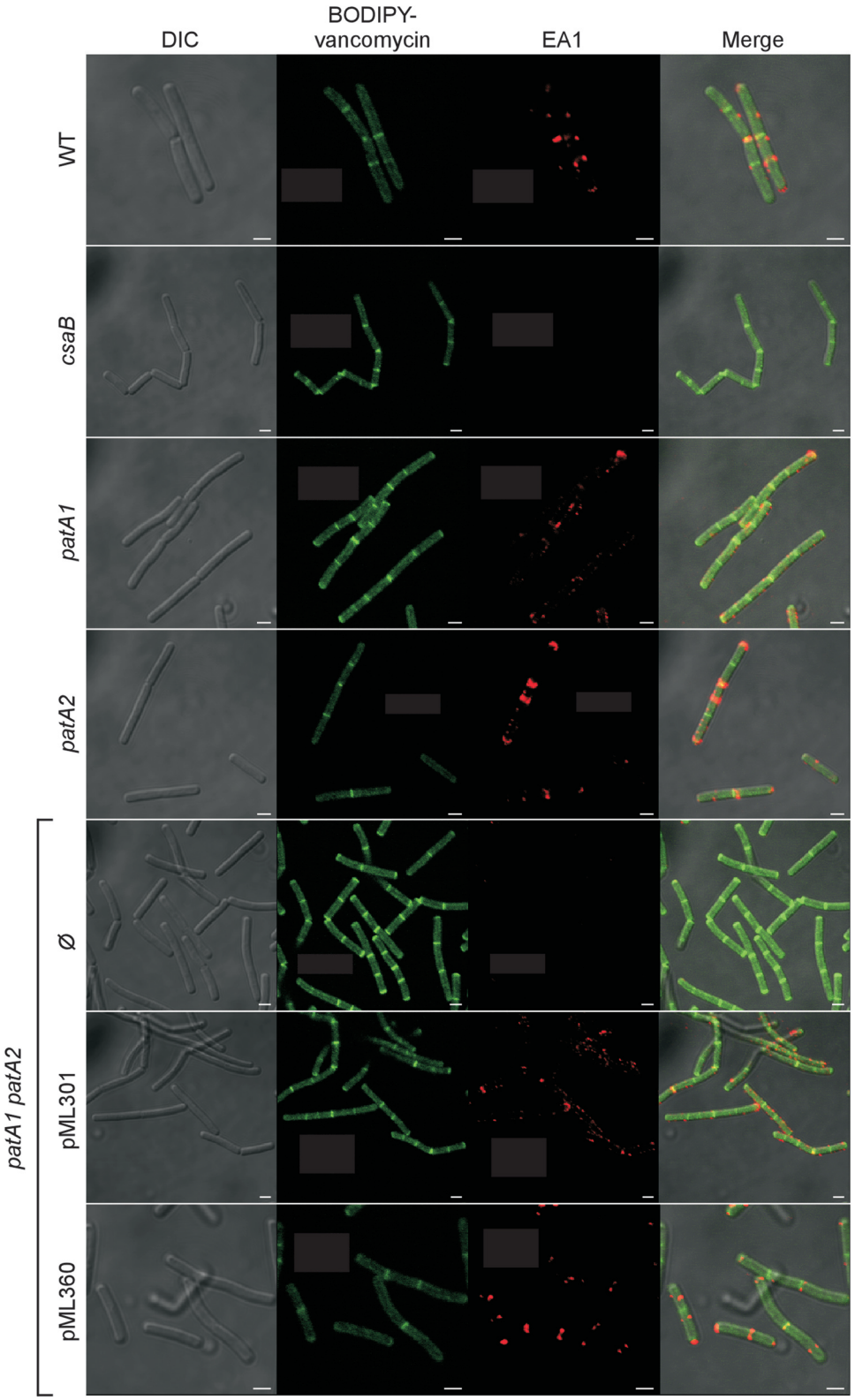

FIG 8 Localization of the S-layer protein EA1 in the envelope of wild-type, *csaB*, *patA1*, *patA2*, and *patA1 patA2 B. anthracis* strains. Spores from wild-type and mutant *B. anthracis* strains were diluted into BHI broth, and germinated bacilli were incubated for 3 h. Vegetative forms were fixed in 4% buffered formalin. Differential interference contrast (DIC) and fluorescence microscopy with BODIPY-vancomycin or rabbit polyclonal antibodies staining against the S-layer protein EA1 followed by secondary antibody DyLight594 conjugate were used to acquire images. Data sets were merged to reveal the location of cell wall septa (BODIPY-vancomycin) and S-layer protein EA1 in wild-type and mutant bacilli. The *patA1 patA2* mutant strain was transformed with plasmid pML301, expressing *patA1* and *patB1*, or pML360, expressing *patA2* and *patB2*, or left untransformed (Ø). Scale bar, 1 μm.

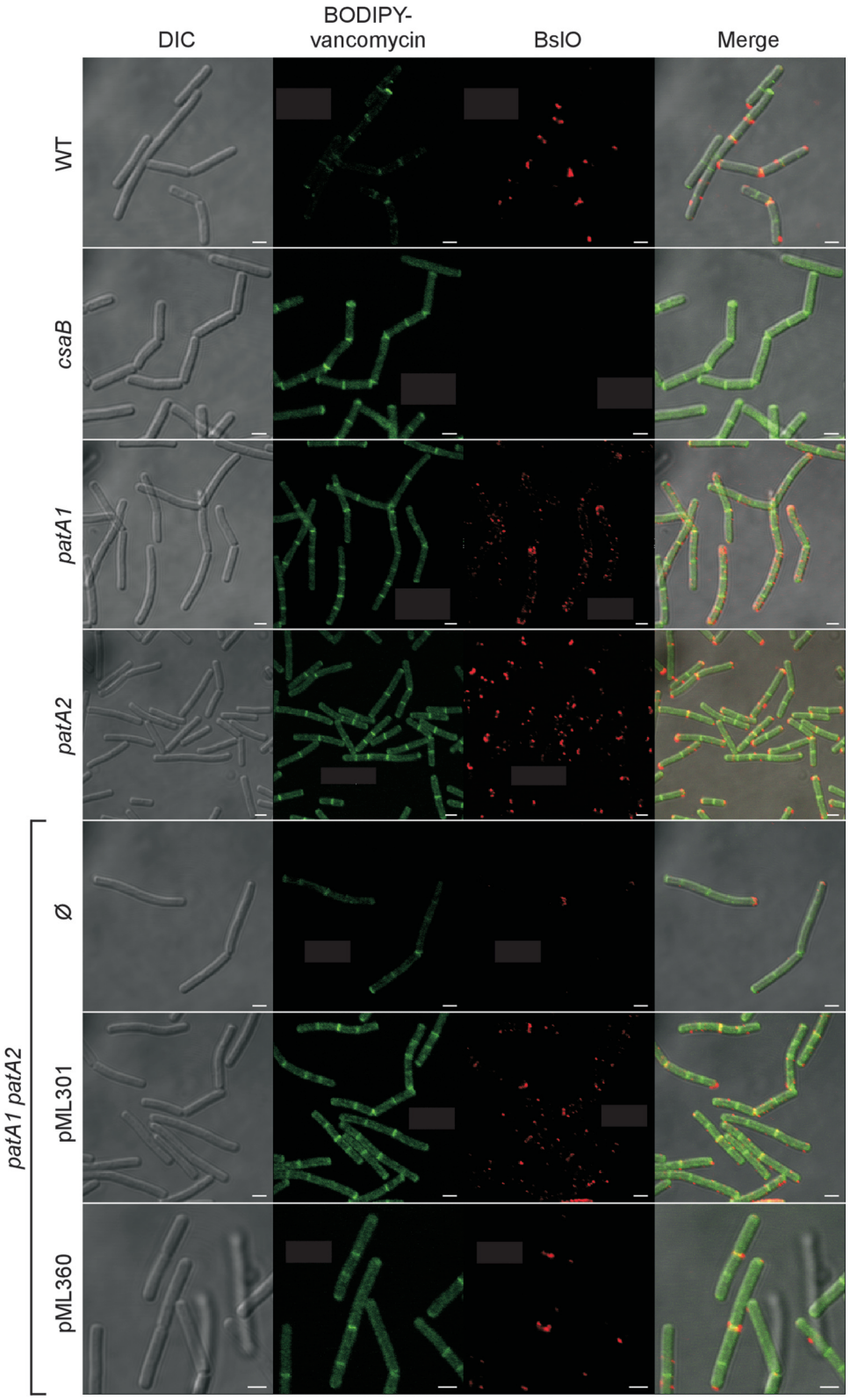

FIG 9 Localization of the S-layer protein EA1 in the envelope of wild-type, *csaB*, *patA1*, *patA2*, and *patA1 patA2 B. anthracis* strains. Spores from wild-type and mutant *B. anthracis* strains were diluted into BHI broth, and germinated bacilli were incubated for 3 h. Vegetative forms were fixed in 4% buffered formalin. Differential interference contrast (DIC) and fluorescence microscopy with BODIPY-vancomycin or rabbit polyclonal antibodies staining against the S-layer-associated protein BslO followed by secondary antibody DyLight594 conjugate were used to acquire images. Data sets were merged to reveal the location of cell wall septa (BODIPY-vancomycin) and the S-layer-associated protein BslO in wild-type and mutant bacilli. The *patA1 patA2* mutant strain was transformed with plasmid pML301, expressing *patA1* and *patB1*, or pML360, expressing *patA2* and *patB2*, or left untransformed (Ø). Scale bar, 1 μm.

bly of the S-layer protein Sap and of the S-layer-associated protein BslO in the bacterial envelope (7, 37). Third, in agreement with this model, *patA1*, *patA2*, and *patA1 patA2* mutants display defects in the deposition of BslO, a murein hydrolase that separates cells from the chains of *B. anthracis* vegetative forms (7). *patA1* and *patA2* likely fulfill nonoverlapping, complementary roles, as the deletion of individual genes causes partial phenotypes for both BslO deposition and chain lengths and as the phenotypic defects are additive for the double mutant strain. Fourth, the *patA1 patA2* mutant strain releases the S-layer protein EA1 as well as BslA and BslO into the extracellular medium. Fifth, the *patA1 patA2* mutant strain is defective in binding $EA1_{SLH}$-mCherry, a reporter harboring the *B. anthracis* SLH domain. Sixth, the SCWP of the *patA1 patA2* mutant strain cannot associate with the SLH domain of the EA1 S-layer protein, and, seventh, the SCWP of the *patA1 patA2* mutant lacks acetyl modifications otherwise found in the SCWP from wild-type bacilli. Taken together, these data suggest that *patA1* and *patA2* function as acetyltransferases that modify the *B. anthracis* cell wall polysaccharide, similar to AlgI of *P. aeruginosa* (26).

Our experimental approach did not investigate the question of whether PatA1 and PatA2 also act to acetylate the peptidoglycan of *B. anthracis*. In this regard, it seems noteworthy that *B. anthracis* harbors homologs of *oatA* and *oatB* (31, 32), acetyltransferases that modify the C-6 hydroxyl of MurNAc or GlcNAc moieties in the repeating disaccharide of peptidoglycan strands (38). Mutants lacking *oatA* or *oatB* harbor defects in cell envelope acetylation but do not display chain length phenotypes (24; also data not shown). These data suggest that the O-6 acetylation of amino sugars in peptidoglycan may not impact S-layer assembly in *B. anthracis*.

Data presented here suggest that *B. anthracis* S-layer assembly does not occur via a mechanism of random deposition for either S-layer proteins or S-layer-associated proteins. The acetylation of the SCWP promotes the deposition of the EA1 S-layer protein and of the BslO murein hydrolase near the cell division septa of vegetative forms. If one entertained a model whereby SCWP acetylation were a prerequisite for association with the SLH domains of EA1 and BslO, but not for the SLH domain of Sap, this would imply that SCWP acetylation must be restricted to the cell division septa. If so, one could assume that PatA1 and PatA2 may also be deposited near cell division septa. Alternative possibilities exist when we take into account the recent discovery that the S-layer proteins (Sap and EA1), but not the BSLs, travel via a dedicated secretory pathway across the bacterial envelope to promote S-layer assembly (37). The subcellular location of the secretion genes, SecA2 and SlaP, is not yet known; however, these translocases could contribute to the overall mechanism of S-layer assembly that also takes into account the mechanisms of S-layer acetylation described here.

Mutations in *B. anthracis csaB*, *patA1*, *patA2*, *sap*, *secA2*, and *slaP* affect the deposition of BslO at cell division septa and the chain length of vegetative bacilli (5, 7, 14, 37); however, these mutations do not affect *B. anthracis* autolysis, as has been reported for the cell separation active murein hydrolases of the Gram-positive microbe *Staphylococcus aureus* (39–41).

ACKNOWLEDGMENTS

We thank members of our laboratory for discussion and comments on the manuscript.

J.M.L. is a trainee of the National Institutes of Health Medical Scientist Training Program at the University of Chicago (grant GM07281).This work was supported by a grant from the National Institute of Allergy and Infectious Diseases (NIAID), Infectious Disease Branch (AI069227 to O.S. and D.M.M.). We acknowledge membership within and support from the Region V Great Lakes Regional Center of Excellence in Biodefense and Emerging Infectious Diseases Consortium (NIAID Award 1-U54-AI-057153).

REFERENCES

1. **Koch R.** 1876. Die Ätiologie der Milzbrand-Krankheit, begründet auf die Entwicklungsgeschichte des *Bacillus anthracis*. Beitr. Biol. Pflanz. **2**:277–310.
2. **Marraffini LA, Schneewind O.** 2006. Targeting proteins to the cell wall of sporulating *Bacillus anthracis*. Mol. Microbiol. **62**:1402–1417.
3. **Candela T, Fouet A.** 2006. Poly-gamma-glutamate in bacteria. Mol. Microbiol. **60**:1091–1098.
4. **Richter GS, Anderson VJ, Garufi G, Lu L, Joachimiak A, He C, Schneewind O, Missiakas D.** 2009. Capsule anchoring in *Bacillus anthracis* occurs by a transpeptidation mechanism that is inhibited by capsidin. Mol. Microbiol. **71**:404–420.
5. **Anderson VJ, Kern JW, McCool JW, Schneewind O, Missiakas DM.** 2011. The SLH domain protein BslO is a determinant of *Bacillus anthracis* chain length. Mol. Microbiol. **81**:192–205.
6. **Ruthel G, Ribot WJ, Bavari S, Hoover T.** 2004. Time-lapse confocal imaging of development of *Bacillus anthracis* in macrophages. J. Infect. Dis. **189**:1313–1316.
7. **Kern VJ, Kern JW, Theriot JA, Schneewind O, Missiakas DM.** 2012. Surface (S)-layer proteins Sap and EA1 govern the binding of the S-layer associated protein BslO at the cell septa of *Bacillus anthracis*. J. Bacteriol. **194**:3833–3840.
8. **Mesnage S, Tosi-Couture E, Mock M, Gounon P, Fouet A.** 1997. Molecular characterization of the *Bacillus anthracis* main S-layer component: evidence that it is the major cell-associated antigen. Mol. Microbiol. **23**:1147–1155.
9. **Etienne-Toumelin I, Sirard JC, Duflot E, Mock M, Fouet A.** 1995. Characterization of the *Bacillus anthracis* S-layer: cloning and sequencing of the structural gene. J. Bacteriol. **177**:614–620.
10. **Kern JW, Schneewind O.** 2008. BslA, a pXO1-encoded adhesin of *Bacillus anthracis*. Mol. Microbiol. **68**:504–515.
11. **Tarlovsky Y, Fabian M, Solomaha E, Honsa E, Olson JS, Maresso AW.** 2010. A *Bacillus anthracis* S-layer homology protein that binds heme and mediates heme delivery to IsdC. J. Bacteriol. **192**:3503–3511.
12. **Kern JW, Schneewind O.** 2010. BslA, the S-layer adhesin of *Bacillus anthracis*, is a virulence factor for anthrax pathogenesis. Mol. Microbiol. **75**:324–332.
13. **Mesnage S, Fontaine T, Mignot T, Delepierre M, Mock M, Fouet A.** 2000. Bacterial SLH domain proteins are non-covalently anchored to the cell surface via a conserved mechanism involving wall polysaccharide pyruvylation. EMBO J. **19**:4473–4484.
14. **Kern J, Ryan C, Faull K, Schneewind O.** 2010. *Bacillus anthracis* surface-layer proteins assemble by binding to the secondary cell wall polysaccharide in a manner that requires *csaB* and *tagO*. J. Mol. Biol. **401**:757–775.
15. **Kern JW, Wilton R, Zhang R, Binkowski A, Joachimiak A, Schneewind O.** 2011. Structure of the SLH domains from *Bacillus anthracis* surface array protein. J. Biol. Chem. **286**:26042–26049.
16. **Choudhury B, Leoff C, Saile E, Wilkins P, Quinn CP, Kannenberg EL, Carlson RW.** 2006. The structure of the major cell wall polysaccharide of *Bacillus anthracis* is species specific. J. Biol. Chem. **281**:27932–27941.
17. **Kojima N, Arakai Y, Ito E.** 1985. Structure of the linkage units between ribitol teichoic acids and peptidoglycan. J. Bacteriol. **161**:299–306.
18. **Forsberg LS, Abshire TG, Friedlander A, Quinn CP, Kannenberg EL, Carlson RW.** 2012. Localization and structural analysis of a conserved pyruvylated epitope in *Bacillus anthracis* secondary cell wall polysaccharides and characterization of the galactose deficient wall polysaccharide from avirulent *B. anthracis* CDC 684. Glycobiology **22**:1103–1117.
19. **Okinaka RT, Price EP, Wolken SR, Gruendike JM, Chung WK, Pearson T, Xie G, Munk C, Hill K, Challacombe J, Ivins BE, Schupp JM, Beckstrom-Sternberg SM, Friedlander A, Keim P.** 2011. An attenuated strain of *Bacillus anthracis* (CDC 684) has a large chromosomal inversion and altered growth kinetics. BMC Genomics **12**:477–490.
20. **Ezzell JWJ, Abshire TG, Little SF, Lidgerding BC, Brown C.** 1990. Identification of *Bacillus anthracis* by using monoclonal antibody to cell

wall galactose-*N*-acetylglucosamine polysaccharide. J. Clin. Microbiol. **28**: 223–231.
21. **Forsberg LS, Choudhury B, Leoff C, Marston CK, Hoffmaster AR, Saile E, Quinn CP, Kannenberg EL, Carlson RW.** 2011. Secondary cell wall polysaccharides from *Bacillus cereus* strains G9241, 03BB87 and 03BB102 causing fatal pneumonia share similar glycosyl structures with the polysaccharides from *Bacillus anthracis*. Glycobiology **21**:934–948.
22. **Leoff C, Saile E, Sue D, Wilkins PP, Quinn CP, Carlson RW, Kannenberg EL.** 2008. Cell wall carbohydrate compositions of strains from *Bacillus cereus* group of species correlate with phylogenetic relatedness. J. Bacteriol. **190**:112–121.
23. **Leoff C, Saile E, Rauvolfova J, Quinn C, Hoffmaster AR, Zhong W, Mehta AS, Boons GJ, Carlson RW, Kannenberg EL.** 2009. Secondary cell wall polysaccharides of *Bacillus anthracis* are antigens that contain specific epitopes which cross-react with three pathogenic *Bacillus cereus* strains that caused severe disease, and other epitopes common to all the *Bacillus cereus* strains tested. Glycobiology **19**:665–673.
24. **Laaberki M-H, Pfeffer J, Clarke AJ, Dworkin J.** 2011. O-Acetylation of peptidoglycan is required for proper cell separation and S-layer anchoring in *Bacillus anthracis*. J. Biol. Chem. **286**:5278–5288.
25. **Hofmann K.** 2000. A superfamily of membrane-bound *O*-acyltransferases with implications for Wnt signaling. Trends Biochem. Sci. **25**:111–112.
26. **Franklin MJ, Ohman DE.** 1996. Identification of *algI* and *algJ* in the *Pseudomonas aeruginosa* alginate biosynthetic gene cluster which are required for alginate O acetylation. J. Bacteriol. **178**:2186–2195.
27. **Franklin MJ, Ohman DE.** 2002. Mutant analysis and cellular localization of the AlgI, AlgJ, and AlgF proteins required for O acetylation of alginate in *Pseudomonas aeruginosa*. J. Bacteriol. **184**:3000–3007.
28. **Weadge JT, Pfeffer JM, Clarke AJ.** 2005. Identification of a new family of enzymes with potential *O*-acetylpeptidoglycan esterase activity in both Gram-positive and Gram-negative bacteria. BMC Microbiol. **5**:49. doi:10.1186/1471-2180-5-49.
29. **Weadge JT, Clarke AJ.** 2006. Identification and characterization of *O*-acetylpeptidoglycan esterase: a novel enzyme discovered in *Neisseria gonorrhoeae*. Biochemistry **45**:839–851.
30. **Dillard JP, Hackett KT.** 2005. Mutations affecting peptidoglycan acetylation in *Neisseria gonorrhoeae* and *Neisseria meningitidis*. Infect. Immun. **73**:5697–5705.
31. **Bera A, Herbert S, Jakob A, Vollmer W, Götz F.** 2005. Why are pathogenic staphylococci so lysozyme resistant? The peptidoglycan *O*-acetyltransferase OatA is the major determinant for lysozyme resistance of *Staphylococcus aureus*. Mol. Microbiol. **55**:778–787.
32. **Bera A, Biswas R, Herbert S, Götz F.** 2006. The presence of peptidoglycan *O*-acetyltransferase in various staphylococcal species correlates with lysozyme resistance and pathogenicity. Infect. Immun. **74**:4598–4604.
33. **Aubry C, Goulard C, Nahori M, Cayet N, Decalf J, Sachse M, Boneca I, Cossart P, Dussurget O.** 2011. OatA, a peptidoglycan *O*-acetyltransferase involved in *Listeria monocytogenes* immune escape, is critical for virulence. J. Infect. Dis. **204**:731–740.
34. **Bernard E, Rolain T, Courtin P, Guillot A, Langella P, Hols P, Chapot-Chartier MP.** 2011. Characterization of O-acetylation of *N*-acetylglucosamine: a novel structural variation of bacterial peptidoglycan. J. Biol. Chem. **286**:23950–23958.
35. **Dunn AK, Handelsman J.** 1999. A vector for promoter trapping in *Bacillus cereus*. Gene **226**:297–305.
36. **Kim HU, Goepfert JM.** 1974. A sporulation medium for *Bacillus anthracis*. J. Appl. Bacteriol. **37**:265–267.
37. **Nguyen-Mau S-M, Oh SY, Kern V, Missiakas D, Schneewind O.** 2012. Secretion genes as determinants of *Bacillus anthracis* chain length. J. Bacteriol. **194**:3841–3850.
38. **Ghuysen JM, Strominger JL.** 1963. Structure of the cell wall of *Staphylococcus aureus*, strain Copenhagen. II. Separation and structure of the disaccharides. Biochemistry **2**:1119–1125.
39. **Kajimura J, Fujiwara T, Yamada S, Suzawa Y, Nishida T, Oyamada Y, Hayashi I, Yamagishi J, Komatsuzawa H, Sugai M.** 2005. Identification and molecular characterization of an *N*-acetylmuramyl-L-alanine amidase Sle1 involved in cell separation of *Staphylococcus aureus*. Mol. Microbiol. **58**:1087–1101.
40. **Yamada S, Sugai M, Komatsuzawa H, Nakashima S, Oshida T, Matsumoto A, Suginaka H.** 1996. An autolysin ring associated with cell separation of *Staphylococcus aureus*. J. Bacteriol. **178**:1565–1571.
41. **Oshida T, Sugai M, Komatsuzawa H, Hong YM, Suginaka H, Tomasz A.** 1995. A *Staphylococcus aureus* autolysin that has an *N*-acetylmuramoyl-L-alanine amidase domain and an endo-β-*N*-acetylglucosaminidase domain: cloning, sequence analysis, and characterization. Proc. Natl. Acad. Sci. U. S. A. **92**:285–289.
42. **Vodkin MH, Leppla SH.** 1983. Cloning of the protective antigen gene of *Bacillus anthracis*. Cell **34**:693–697.
43. **Williams RC, Rees ML, Jacobs MF, Praqai Z, Thwaite JE, Baillie LW, Emmerson PT, Harwood CR.** 2003. Production of *Bacillus anthracis* protective antigen is dependent on extracellular chaperone, PrsA. J. Biol. Chem. **278**:18056–18062.